Modeling and Identification of Permanent Magnet Synchronous Motor via Deterministic Learning

WEI YU [1], HENGHUI LIANG[1], XUNDE DONG [2], AND YING LUO[1,3], (Member, IEEE)
[1]School of Mechatronic Engineering and Automation, Foshan University, Foshan 528225, China
[2]School of Automation Science and Engineering, South China University of Technology, Guangzhou 510641, China
[3]Department of Mechanical Science and Engineering, Huazhong University of Science and Technology, Wuhan 430074, China

Corresponding author: Xunde Dong (audxd@scut.edu.cn)

ABSTRACT This paper investigates the identification of a permanent magnet synchronous motor (PMSM) velocity servo system based on deterministic learning theory. Unlike most of the existing studies, this study does not identify the system parameters, but rather the system dynamics. System dynamics is the fundamental knowledge of the PMSM system and contains all the information about the system parameters, various uncertainties, and the system structure. The accurate modeling of the various uncertainties is important to improve the control performance of the controller. In this study, the dynamics of the PMSM system containing various uncertainties are identified based on the system state. Firstly, the system state of the PMSM is measured, and then a suitable RBF neural network is designed based on it. The RBF neural network is used to construct a state estimator that takes the motor system as input. The weights of the RBF neural network are updated using the Lyapunov-based weights. As the weights converge, a constant RBF neural network can be obtained, which contains complete information about the system parameters and the various uncertainties of the motor system. We use the proposed method to identify the simulated and real-time PMSM velocity servo systems separately, and the identification results show the effectiveness and feasibility of the proposed method.

INDEX TERMS Deterministic learning, permanent magnet synchronous motor, uncertainties, system identification.

I. INTRODUCTION

Permanent magnet synchronous motor (PMSM) has become the mainstream motor in the fields of active aircraft, electric vehicles and industrial servo drives due to its high torque density, high power density, and high efficiency. It is a typical nonlinear complex system with the general properties of chaotic systems, showing self-similarity, initial value sensitivity, and signal pseudo-random complexity [1]. Synchronous motors contain both AC and DC types in principle, and its dynamic model typically can be treated as the universal model of motors. Therefore, accurate modeling of a permanent magnet synchronous motor has universal significance for general motion control optimization with fault diagnosis and also has a strong application background.

The associate editor coordinating the review of this manuscript and approving it for publication was Jinquan Xu.

PMSM is a multivariable and dynamic time-varying system. The actual control strategy is affected by the uncertainty of the mathematical model of the motor. The most common uncertainty is the electrical parameters in the motor model [2]. In actual control, these variations in electrical parameters will cause inaccurate estimation of various observers, failure of shaft decoupling, control performance, the dynamic and static modeling quality reduction, and even affecting the stability of the motor control system [3]. To accurately identify the parameters of the PMSM to get an accurate motor model and improve the control performance, a variety of PMSM parameter identification methods have appeared, such as model reference adaptive (MRAS) method, state observer method, intelligent identification method and so on.

In [4], the authors used the current model in the PMSM synchronous rotating coordinate system as a reference model

to construct a quadrature axis observer. Based on the error of the reference model and the adjustable model, the quadrature axis current was designed using the Lyapunov stability theory to be identified parametric resistance, quadrature axis inductance, and magnetic flux adaptive law. References [5], [6] used the estimated quadrature axis voltage equation as a reference model and then designed adaptive rules to identify the stator resistance by Lyapunov stability theory. Although the MRAS identification method has been successfully applied in the parameter identification of PMSM [7], [8], the derivation of the adaptive law is mostly carried out under assumptions. It is difficult to determine the adaptive law if multiple parameters are identified simultaneously. Furthermore, the velocity of adjustment and change during parameter identification is slow, which is not suitable for the identification of fast time-varying parameters. The Kalman filter has been successfully applied in the parameter identification of PMSM [9]–[11], but there are still two main problems. One is that the algorithm is complex and computationally intensive. The other is that it requires more assumptions in use and has significant limitations in practical applications.

With the development of intelligent optimization control, many intelligent algorithms appeared in PMSM parameter identification and control, such as Grey wolf optimization algorithm [12], [13], particle swarm algorithm [14], [15], genetic algorithm [16], [17], wavelet algorithm and neural network algorithm [18], [19], etc. For a motor model with known structure but unknown or partially unknown parameters, the problem of identifying motor parameters is transformed into obtaining the optimal solution. Although the intelligent identification algorithm has high accuracy, strong robustness, and fast convergence speed, the algorithm is generally complicated with a large amount of calculation, poor real-time performance, and requires a higher computing capacity. These unfavorable factors hinder the practical application of the intelligent identification algorithm.

Although much research has been done on parameter identification of motor systems, the model structures used in existing studies are generally linear, and the number of parameters to be identified is 3 to 5. It is difficult to accurately model the nonlinear dynamics in the system, especially the various uncertainties. It is worth noting that accurate modeling of uncertainty and its application in controllers can be of great help in improving control performance [20].

Recently, a new algorithm, deterministic learning theory, has been proposed for nonlinear system identification, temporal pattern recognition, and intelligent control of nonlinear systems [21], [22]. The main feature of the deterministic learning approach, compared to existing system identification methods, is the achieved accurate identification of the local true nonlinear system model, which contains information about the system parameters, various uncertainties, and the system structure. Furthermore, the obtained knowledge can be stored and represented by constant RBF neural networks and can be readily used for another similar control task toward guaranteed stability and improved control performance.

In this paper, a method is proposed for the identification of the motor system via deterministic learning. Unlike most of the existing studies, this study does not identify the system parameters, but the system dynamics, which is the fundamental knowledge of the motor system. The system state of the motor is first measured, and then a suitable RBF neural network is designed accordingly. A state estimator is built using the RBF neural network with the system state of the motor as input. The weights of the RBF neural network are updated using Lyapunov-based law. It can be shown that these parameters all converge to a constant value. Thus, a constant RBF neural network can be obtained, which is the dynamics underlying the motor system states and can be used for control, pattern recognition, fault detection, and so on. The information about all system parameters and the structure is also contained in this constant RBF neural network.

The major contributions of this paper include: (1) This method provides accurate identification of the system dynamics of a motor system, rather than the system parameters. System dynamics is the essential characteristic of a motor system and contains all the information of the system, including information of system parameters and various uncertainties; (2) The method is of good practicality, requiring only the state of the system, and is particularly suitable for the identification of real-time motor systems with various uncertainties; (3) The modeling result is expressed as a constant radial basis function (RBF) networks, which can be readily used for another similar control task toward guaranteed stability and improved control performance.

The remainder of the paper is organized as follows. Sections 2 and 3 introduce the dynamic mathematical model of PMSM and deterministic learning, respectively. Section 4 gives the details of the identification method proposed in this paper. Section 5 presents the process and results of the simulation and experimental tests. Section 6 concludes the paper.

II. DYNAMIC MATHEMATICAL MODEL OF PMSM

PMSM is a multi-variable, strongly coupled non-linear system whose electrical parameters affect each other. Therefore, it is difficult to get an accurate PMSM mathematical model. In the actual control of PMSM, the state equation in the d-q two-phase synchronous rotating coordinate system is usually used as a mathematical model. The dynamic equation of a PMSM system in a rotating (d-q) coordinate system can be expressed as follows [23]–[25]:

$$\begin{cases} \dfrac{d\omega}{dt} = -\dfrac{B}{J}\omega + \dfrac{n_p}{J}[(L_d - L_q)i_d i_q + \Psi_r i_q] - \dfrac{T_L}{J} \\ \dfrac{di_q}{dt} = -\dfrac{n_p}{L_q}\Psi_r\omega - \dfrac{R}{L_q}i_q - \dfrac{n_p}{L_q}\omega i_d L_d + \dfrac{u_q}{L_q} \\ \dfrac{di_d}{dt} = \dfrac{n_p}{L_d}\omega i_q L_q - \dfrac{R}{L_d}i_d + \dfrac{u_d}{L_d} \end{cases} \quad (1)$$

where ω, J, R, B, n_p, T_L and Ψ_r are rotor angular velocity, rotor moment of inertia, stator resistance, viscous friction coefficient, pole pair, load torque, and flux linkage,

respectively. i_d and i_q denote $d-$axis and q-axis currents, u_d and u_q represent d-axis and q-axis voltages, L_d and L_q are d-axis and q-axis inductance, respectively. Under different operating conditions, these electrical parameters can be affected by various factors, where the most important factors are the uncertainties.

The system state of a motor system is a time-varying pattern with a recurrent trajectory. It is generated by the motor system and is the manifestation of information about the system parameters, various uncertainties, and system structure, i.e., the system dynamics. In this study, we will identify the dynamics of the system based on the system state, which contains all the information about the system.

III. DETERMINISTIC LEARNING
Deterministic learning theory is a machine learning method recently proposed for the identification and recognition of timing-varying patterns [21]. It was principally developed based on the knowledge of RBF neural networks, adaptive control, and system identification. For a temporal pattern, which is defined as a periodic or recurrent orbit generated by nonlinear dynamical systems, the fundamental knowledge of the temporal pattern can be accurately identified and stored as a time-invariant manner [22], [26].

To be more specific, consider the following dynamical system:

$$\dot{u} = G(u; p), \quad u(t_0) = u_0 \tag{2}$$

where $u = [u_1, \ldots, u_n]^T \in R^n$ is the system state, $G(u; p) = [g_1(u; p), \ldots, g_n(u; p)]^T$ is a continuous but unknown nonlinear function vector, and p is a constant parameter vector.

In order to accurately model the unknown system dynamics $G(u; p)$ underlying a dynamical pattern φ_ζ (a recurrent orbit), the following estimator system is applied:

$$\dot{\hat{u}}_i = -d_i(\hat{u}_i - u_i) + \hat{W}_i^T S_i(u), \tag{3}$$

where u_i and $\hat{u}_i$ are states of (2) and (3) respectively, $d_i > 0$ is a parameter to be designed, RBF neural networks $\hat{W}_i^T S_i(u)$ is used to approximate $g_i(u; p)$, $\hat{W}_i = [w_{i1}, \ldots, w_{iN}]^T \in R^N$ and $S_i(u) = [s_{i1}(\| u - \xi_1 \|), \ldots, s_{iN}(\| u - \xi_N \|)]^T$, ξ_j are distinct points in state space, $s_{ij}(\cdot)$ is Gaussian function.

Subtract Eq.(2) from Eq.(3), the following equation can be obtained:

$$\begin{aligned} \dot{\tilde{u}}_i &= -d_i\tilde{u}_i + \hat{W}_i^T S_i(u) - g_i(u; p) \\ &= -d_i\tilde{u}_i + \tilde{W}_i^T S_i(u) - e_i, \end{aligned} \tag{4}$$

where $\tilde{u}_i = \hat{u}_i - u_i$ is state estimation error, $\tilde{W}_i = \hat{W}_i - W_i^*$, W_i^* is the ideal constant weight vector, $e_i = g_i(u; p) - W_i^{*T} S_i(u)$ is the ideal approximation error. To update $\hat{W}_i$, the following Lyapunov-based learning law was employed:

$$\dot{\hat{W}}_i = -\gamma_i S_i(u)\tilde{u}_i - \sigma_i\gamma_i\hat{W}_i, \tag{5}$$

where $\sigma_i > 0$ is a small constant parameter, $\gamma_i = \gamma_i^T > 0$. It has proved that for almost any temporal pattern (recurrent orbit) φ_ζ, the accurate identification of unknown dynamics

$g_i(u; p)$ along the orbit φ_ζ can be obtained [21], [22], [26] and represented as follows:

$$\begin{aligned} g_i(\varphi_\zeta; p) &= \hat{W}_i^T S_i(\varphi_\zeta) + e_{\zeta i} \\ &= \bar{W}_i^T S_i(\varphi_\zeta) + e_{\zeta i1}, \end{aligned} \tag{6}$$

where $\bar{W}_i = mean_{t \in [t_s, t_f]}\hat{W}_i(t)$, *mean* is the arithmetic mean, $[t_s, t_f]$ is a span of time after the transient process, $e_{\zeta i1} = O(e_{\zeta i}) = O(e_i)$ is the actual modeling error. It indicates the dynamics underlying nearly any temporal pattern can be accurately modeled by applying deterministic learning.

The deterministic learning has shown that for almost every periodic orbit, there always exists an RBF subvector consisting of RBFs centered in a certain neighborhood of the orbit such that a partial PE condition is satisfied. With the satisfaction of the persistent excitation (PE) condition, locally accurate modeling of nonlinear system models along periodic or quasi-periodic trajectories was achieved. While existing nonlinear system identification methods can only guarantee that the state estimation error converges to a small neighborhood of zero, but they cannot perform a system dynamics accurate identification (i.e., there is no guarantee that the weights of the neural networks will converge to their optimal values). This is the main contribution of deterministic learning. Moreover, the acquired knowledge can be stored and represented by a constant RBF neural network and can be readily used for another similar control task.

IV. IDENTIFICATION METHOD
In the section, we will present the method for identifying the PMSM model. For simplicity of notation we denote

$$X = [\omega, i_p, i_d]^T$$

is the system state vector, and

$$p = [R, L_d, L_q, n_p, B, \Psi_r, u_d, u_q]$$

is the system parameter vector, and

$$\begin{cases} F_1(X; p) = -\dfrac{B}{J}\omega + \dfrac{n_p}{J}[(L_d - L_q)i_d i_q + \Psi_r i_q] - \dfrac{T_L}{J} \\ F_2(X; P) = -\dfrac{n_p}{L_q}\Psi_r\omega - \dfrac{R}{L_q}i_q - \dfrac{n_p}{L_q}\omega i_d L_d + \dfrac{u_q}{L_q} \\ F_3(X; p) = \dfrac{n_p}{L_d}\omega i_q L_q - \dfrac{R}{L_d}i_d + \dfrac{u_d}{L_d} \end{cases}$$

then the motor system (1) can be abbreviated as follows:

$$\dot{X} = F(X; p) \tag{7}$$

where $X = [\omega, i_q, i_d]^T$ is the system state, $F(X, p) = [F_1(X; p), F_2(X; p), F_3(X; p)]^T$ is the nonlinear function vector, p is the system parameter vector.

To achieve the locally accurate identification of the system dynamics $F_1(X; p)$, $F_2(X; p)$ and $F_3(X; p)$, we employ the dynamical models using the RBF neural network as follows:

$$\begin{cases} \dot{\hat{\omega}} = -a_1(\hat{\omega} - \omega) + \hat{W}_1^T S_1(X) \\ \dot{\hat{i}}_q = -a_2(\hat{i}_q - i_q) + \hat{W}_2^T S_2(X) \\ \dot{\hat{i}}_d = -a_3(\hat{i}_d - i_d) + \hat{W}_3^T S_3(X) \end{cases} \tag{8}$$

where $\hat{\omega}$, $\hat{i}_q$ and $\hat{i}_d$ are the estimation of ω, i_q, i_d, respectively, $a_i > 0$ $(i = 1, 2, 3)$ is constant parameter to be designed, $\hat{W}_i^T S_i(X)$ is the RBF neural networks to approximate $F_i(X; p)$ $(i = 1, 2, 3)$.

From Eqs. (7) and (8), the derivative of the state estimation errors $e_1 = \hat{\omega} - \omega$, $e_2 = \hat{i}_q - i_q$ and $e_3 = \hat{i}_d - i_d$ satisfy

$$
\begin{cases}
\dot{e}_1 = -a_1 e_1 + \hat{W}_1^T S_1(X) - F_1(X; p) \\
\quad = -a_1 e_1 + \widetilde{W}_1^T S_1(X) - \epsilon_1 \\
\dot{e}_2 = -a_2 e_2 + \hat{W}_2^T S_2(X) - F_2(X; p) \\
\quad = -a_2 e_2 + \widetilde{W}_2^T S_2(X) - \epsilon_2 \\
\dot{e}_3 = -a_3 e_3 + \hat{W}_3^T S_3(X) - F_3(X; p) \\
\quad = -a_3 e_3 + \widetilde{W}_3^T S_3(X) - \epsilon_3
\end{cases}
\tag{9}
$$

where $\widetilde{W}_i = \hat{W}_i - W_i^*$, $\hat{W}_i$ is the estimation of W_i^*, W_i^* is the the optimal value of $\hat{W}_i$, $\epsilon_i = F_i(X; p) - W_i^{*T} S_i(X)$ $(i = 1, 2, 3)$ are the ideal approximation errors. The weight estimates $\hat{W}_i (i = 1, 2, 3)$ are updated by the following law:

$$
\dot{\hat{W}}_i = \dot{\widetilde{W}}_i = -\Gamma_i S_i(X) e_i - \sigma_i \Gamma_i \hat{W}_i \tag{10}
$$

where $\Gamma_i = \Gamma_i^T > 0$, and $\sigma_i > 0$ are small values.

It can be indicated from the following theorem that the accurate identification of $F_i(X; p)$ $(i = 1, 2, 3)$ can be obtained along a recurrent trajectory of the motor system (1).

Theorem 1: Consider the adaptive system composed by the motor system (7), the dynamical model (8), and the updating law (10), the following conclusions can be drawn: (i) all signals in the adaptive system remain uniformly bounded, the state estimation error e_i $(i = 1, 2, 3)$ converges to a small neighborhood of zero, and the neural weight estimate $\hat{W}_{\zeta i}$ (as in (16)) converges to a small neighborhood of its optimal value $\hat{W}_{\zeta i}^*$ $(i = 1, 2, 3)$; (ii) locally accurate approximation of $F_i(X; p)$ $(i = 1, 2, 3)$ can be achieved along the recurrent trajectory $\phi(X)$ of the motor system (7).

Proof: (i) Consider the following Lyapunov function candidate:

$$
V_i = \frac{1}{2}(e_i^2 + \widetilde{W}_i^T \Gamma_i^{-1} \widetilde{W}_i), \quad i = 1, 2, 3 \tag{11}
$$

Take the derivative of V_i,

$$
\begin{aligned}
\dot{V}_i &= e_i \dot{e}_i + \widetilde{W}_i^T \Gamma_i^{-1} \dot{\widetilde{W}}_i \\
&= -a_i e_i^2 - e_i \epsilon_i - \sigma_i \widetilde{W}_i^T \hat{W}_i
\end{aligned}
\tag{12}
$$

Let $a_i = a_{i1} + a_{i2}$ with $a_{i1}, a_{i2} > 0$. Because

$$
\begin{cases}
-a_{i2} e_i^2 - e_i \epsilon_i \leq \dfrac{\epsilon_i^2}{4a_{i2}} \\
-\sigma_i \widetilde{W}_i^T \hat{W}_i \leq -\sigma_i \|\widetilde{W}_i\|^2 + \sigma_i \|\widetilde{W}_i\| \|W_i^*\| \\
\qquad\qquad \leq -\dfrac{\sigma_i \|\widetilde{W}_i\|^2}{2} + \dfrac{\sigma_i \|\widetilde{W}_i^*\|^2}{2}
\end{cases}
\tag{13}
$$

it follows that

$$
\dot{V}_i \leq -a_{i1} e_i^2 - \frac{\sigma_i \|\widetilde{W}_i\|^2}{2} + \frac{\sigma_i \|\widetilde{W}_i^*\|^2}{2} + \frac{\epsilon_i^2}{4a_{i2}} \tag{14}
$$

Clearly, $\dot{V}_i$ is negative definite when

$$
|e_i| > \frac{\epsilon_i}{2\sqrt{a_{i1} a_{i2}}} + \sqrt{\frac{\sigma_i}{2a_{i1}}} \|W_i^*\|
$$

or

$$
\|\widetilde{W}_i\| > \frac{\epsilon_i}{\sqrt{2\sigma_i a_{i2}}} + \|W_i^*\|
$$

That is, e_i and $\widetilde{W}_i$ are uniformly bounded

$$
\begin{cases}
|e_i| \leq \dfrac{\epsilon_i}{2\sqrt{a_{i1} a_{i2}}} + \sqrt{\dfrac{\sigma_i}{2a_{i1}}} \|W_i^*\| \\
\|\widetilde{W}_i\| \leq \dfrac{\epsilon_i}{\sqrt{2\sigma_i a_{i2}}} + \|W_i^*\|
\end{cases}
\tag{15}
$$

Based on the locally properties of RBF neural network, we describe Eq. (9) and Eq. (10) in the following form:

$$
\begin{bmatrix} \dot{e}_i \\ \dot{\widetilde{W}}_{\zeta i} \end{bmatrix} = \begin{bmatrix} -a_i & S_{\zeta i}(U)^T \\ -\Gamma_{\zeta i} S_{\zeta i}(U) & 0 \end{bmatrix} \begin{bmatrix} e_i \\ \widetilde{W}_{\zeta i} \end{bmatrix} + \begin{bmatrix} -\epsilon_{\zeta i} \\ -\sigma_i \Gamma_{\zeta i} \hat{W}_{\zeta i} \end{bmatrix}
\tag{16}
$$

and

$$
\dot{\hat{W}}_{\bar{\zeta} i} = \dot{\widetilde{W}}_{\bar{\zeta} i} = -\Gamma_{\bar{\zeta} i} S_{\bar{\zeta} i} - \sigma_i \Gamma_{\bar{\zeta} i} \hat{W}_{\bar{\zeta} i} \tag{17}
$$

where $(\cdot)_\zeta$, $(\cdot)_{\bar{\zeta}}$ represent the area close to and far away from the trajectory $\phi(X)$, respectively. $S_{\zeta i}$ is a subvector of S_i, $\hat{W}_{\zeta i}$ is the corresponding weight subvector. $\epsilon_{\zeta i} = O(\epsilon_i)$ is the neural network approximation error along the trajectory $\phi(X)$. According to the nature of RBF neural networks, any recurrent trajectory can satisfy a partial persistent excitation (PE) condition of the corresponding RBF subvector. Since the trajectory $\phi(X)$ generated by the motor model (7) is recurrent, $S_{\zeta i}$ satisfies the PE condition. Based on Lemma 2 in reference [27], the origin $(e_i, \widetilde{W}_{\zeta i}) = 0$ of the nominal part of the system (16) is exponentially stable. Since $\epsilon_{\zeta i} = O(\epsilon_i)$ and $\sigma_i \Gamma_{\zeta i} \hat{W}_{\zeta i}$ can be made small by choosing a sufficiently σ_i, by using Lemma 3 in [27], the state error e_i and $\widetilde{W}_{\zeta i}$ both converge exponentially to some small neighborhoods of zero, and the size of the neighborhoods being determined by ϵ_i^* and $\sigma_i \|\Gamma_{\zeta i} W_{\zeta i}^*\|$, respectively.

(ii) The convergence of $\hat{W}_{\zeta i}$ to be in a small neighborhood of $W_{\zeta i}^*$ means that along the trajectory $\phi(X)$,

$$
\begin{aligned}
F_i(X; p) &= W_{\zeta i}^{*T} S_{\zeta i} + \epsilon_{\zeta i} \\
&= \hat{W}_{\zeta i}^T S_{\zeta i} - \widetilde{W}_{\zeta i}^T S_{\zeta i} + \epsilon_{\zeta i} \\
&= \hat{W}_{\zeta i}^T S_{\zeta i} + \epsilon_{\zeta l_i}
\end{aligned}
\tag{18}
$$

where $\epsilon_{\zeta l_i} = \epsilon_{\zeta i} - \widetilde{W}_{\zeta i}^T S_{\zeta i} = O(\epsilon_{\zeta i})$.

Based on the convergence result, a constant vector of neural weights can be obtained according to the following formula:

$$
\bar{W}_{\zeta i} = mean_{t \in [t_a, t_b]} \hat{W}_{\zeta i}
$$

where "mean" is the arithmetic mean, and $[t_a, t_b]$ represents a piece of time segment after the transient process. So, we have that

$$
F_i(X; p) = \hat{W}_{\zeta i}^T S_{\zeta i} + \epsilon_{\zeta i_1} = \bar{W}_{\zeta i}^T S_{\zeta i} + \epsilon_{\zeta i_2} \tag{19}
$$

where $\epsilon_{\zeta i_2} = O(\epsilon_{\zeta i_1}) = O(\epsilon_{\zeta i})$.

On the other hand, for neurons far away from the trajectory $\phi(X)$, $|S_{\bar{\zeta}i}|$ will become very small due to the localization characteristic of RBFs, so the activation and update of the neural weights $\bar{W}_{\bar{\zeta}i}$ is very weak. For the initial value $\hat{W}_i(0) = 0$, both $\hat{W}_{\bar{\zeta}i}$ and $\hat{W}_{\bar{\zeta}i}^T S_{\bar{\zeta}i}$, as well as $\bar{W}_{\bar{\zeta}i}$ and $\bar{W}_{\bar{\zeta}i}^T S_{\bar{\zeta}i}$ will remain very small (i.e., still in a small neighborhood of zero). These mean that the entire RBF neural network $W_i^T S_i$ can approximate $F_i(X; p)$ along the trajectory $\phi(X)$:

$$
\begin{aligned}
F_i(X; p) &= \bar{W}_{\zeta i}^T S_{\zeta i} + \epsilon_{\zeta i_2} \\
&= \bar{W}_{\zeta i}^T S_{\zeta i} + \bar{W}_{\bar{\zeta}i}^T S_{\bar{\zeta}i} + \epsilon_{\zeta i_2} - \bar{W}_{\bar{\zeta}i}^T S_{\bar{\zeta}i} \\
&= \bar{W}_i^T S_i + \epsilon_{i_e}
\end{aligned}
\tag{20}
$$

where $\epsilon_{i_e} = \epsilon_{\zeta i_2} - \bar{W}_{\bar{\zeta}i}^T S_{\bar{\zeta}i} = O(\epsilon_{\zeta i_2}) = O(\epsilon_i)$. It implies that accurate identification of the motor system to the desired error level ϵ_i is achieved by using the entire RBF neural network in a local region along the recurrent trajectory $\phi(X)$ of the motor system.

V. SYSTEM IDENTIFICATION FOR THE DYNAMICS MATHEMATICAL MODEL

A. SIMULATION AND EXPERIMENTAL PLATFORM

The PMSM first runs under a normal steady-state condition, and then a pseudo-random binary signal (PRBS) is added to the PMSM after a prescribed time. The length and period of the PRBS signal are designed based on the cut-off frequency of the PMSM. With this input data set, the PMSM is fully excited, which allows the model to recognize the complete system behavior. If control $i_d = 0$, the PMSM will be decoupled, and we can control the PMSM as easily as a DC motor.

Space vector pulse width modulation (SVPWM) is a special switching scheme of a 3-phase power converter with six power transistors. We apply SVPWM to approximate the reference voltage and combine it with eight basic space vectors [28]. Modeling details of the SVPWM design can be found in [29]. The 3-phase inverter consists of three groups of IGBT power transistors. Every group is composed of upper and lower two transistors, the six IGBT power transistors are controlled by the PWM1-PWM6 signals from the SVPWM module, and the outputs of the inverter connect to the 3-phase inputs of the motor. The PMSM is driven by a conventional voltage-source inverter. The two input currents of the PMSM (i_a and i_b) are measured by the inverter and sent to the DSP controller via two analog-to-digital converters (ADCs).

Theoretically, PMSM-driven field-oriented control allows for independent control of motor torque and magnetic flux, as in DC motor operation. In other words, torque and magnetic flux are decoupled from each other. Rotor position requires a variable conversion from a stationary reference frame to a synchronously rotating reference frame. Due to this conversion (i.e., park transformation), the q-axis current will control the torque, while the d-axis current is forced to zero. Therefore, the key module of this system is the rotor position information from the QEP encoder. The overall flow diagram

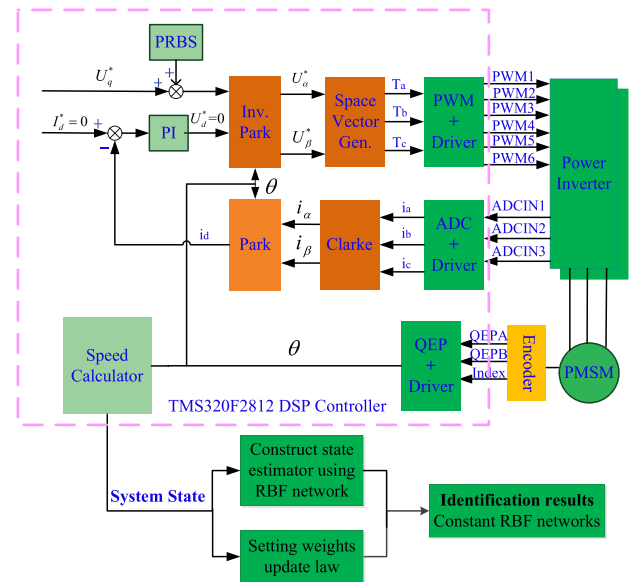of the simulation and experimental platform implementation is shown in Figure 1.

FIGURE 1. The flow diagram of the simulation and experimental platform implementation.

FIGURE 2. Experimental Set-up.

The PMSM real-time velocity control experimental platform shown in Figure 2 will be used for accurate identification and experimental verification. The PMSM is controlled by a servo drive and connected to a computer for signal monitoring using a Joint Test Action Group (JTAG) emulator interface. The code composer studio (CCS) software tool is used for online tuning and debugging. The control board uses a Texas Instruments TMS320F2812 DSP control unit. The two-phase current signal is sampled from the current transducer and used as current feedback for closed-loop control. The speed feedback signal is obtained from the encoder output as speed closed-loop control.

B. NUMERICAL EXPERIMENTS

The following numerical simulation is conducted to show the effectiveness and feasibility of the method. Referring to

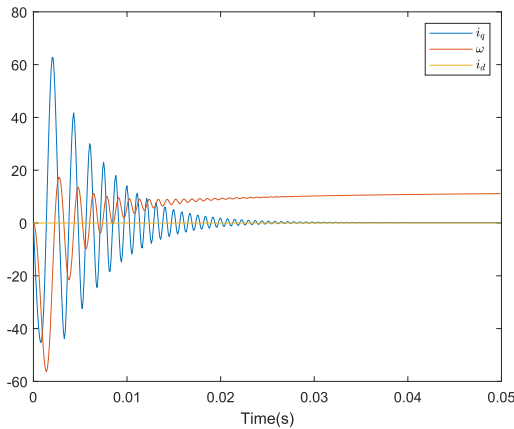Figure 1, if the control $i_d = 0$, the PMSM will be decoupled and can be controlled as easily as a DC motor.

FIGURE 3. The numerical solution of Eq. (7).

The numerical solutions are obtained from the Eq. (7) (as shown in Figure 3) with the following parameters: $n_p = 4$, $\Psi_r = 0.892wb$, $L_d = L_q = 0.003H$, $J = 0.00251kg \cdot m^2$, $R = 1.32ohm$, $B = 0.025$, $T_L = 0.1N \cdot m$, and

$$\begin{bmatrix} u_d(t) \\ u_q(t) \end{bmatrix} = \sqrt{\frac{2}{3}} \begin{bmatrix} \cos(8\pi\omega t) & \sin(8\pi\omega t) \\ -\sin(8\pi\omega t) & \cos(8\pi\omega t) \end{bmatrix}$$
$$\cdot \begin{bmatrix} 1 & -\frac{1}{2} & -\frac{1}{2} \\ 0 & \frac{\sqrt{3}}{2} & -\frac{\sqrt{3}}{2} \end{bmatrix} \cdot \begin{bmatrix} 220\sin(100\pi t) \\ 220\sin(100\pi t - 2\pi/3) \\ 220\sin(100\pi t + 2\pi/3) \end{bmatrix}$$

The dynamical model employing RBF neural networks Eq. (8) are used to identify the unknown system dynamics $F_i(X; p)(i = 2, 3)$ in Eq. (7). The RBF neural network $\hat{W}_i^T S_i(X)(i = 2, 3)$ is constructed in a regular lattice, with nodes $N = 408$, the centers evenly placed on $[-50, 65] \times [-60, 20]$, and the width is 5. The weights of the RBF neural networks are updated online according to Eq. (10). The initial weights $\hat{W}_i(0) = 0$. Figure 4 shows the convergence of the neural network weights W_1 and W_2. The NN approximations of $F_2(X; p)$ and $F_3(X; p)$ in the time domain are shown in Figure 5. It can be seen that the accurate identification of the system dynamics is achieved. From these figures, we can see that accurate approximation of dynamics $F_2(X; p)$ and $F_3(X; p)$ are indeed achieved. The accurate NN approximations can be considered as partially true system dynamics $F_2(X; p)$ and $F_3(X; p)$ stored in constant RBF neural networks $\bar{W}_2^T S_2(X)$ and $\bar{W}_3^T S_3(X)$. Correspondingly, the accurate identification of the PMSM velocity response can also be achieved. As an example, the identification results of PMSM with PRBS is presented.

The PMSM first runs at a normal steady-state condition. After a prescribed time $T_s = 0.2s$ has elapsed, the PRBS is sent to the PMSM. The PMSM velocity response with the input PRBS and its identification results are shown in Figure 6, where the blue line is the PMSM velocity response with PRBS, the red line is the identification results. We can
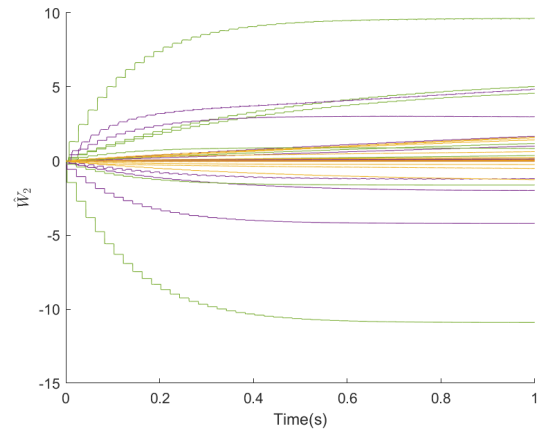
(a) Parameter convergence: $\hat{W}_2$
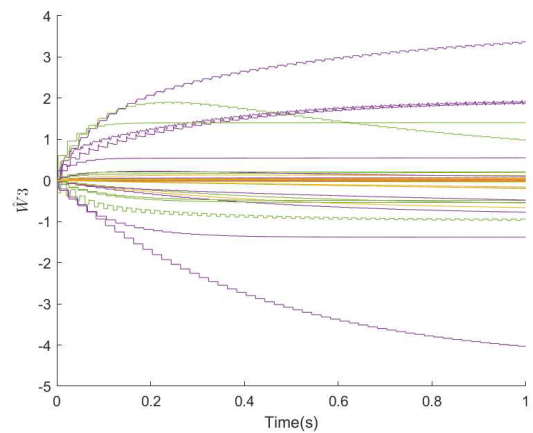
(b) Parameter convergence: $\hat{W}_3$

FIGURE 4. The convergence of the neural network weights.

see that the accurate identification of the PMSM velocity response is indeed achieved.

TABLE 1. Nominal parameters of the PMSM in experiment.

| Rated power	1 (kw)
Rotor flux	0.892 (wb)
Rated torque	4.7 (N.m/Arms)
Armature resistance	1.32 (ohm)
Mechanical time constant (T_m)	5.9 (ms)
Electrical time constant(T_l)	4.5 (ms)
Number of poles	8
Moment of inertia	0.00251 (kg.m^2)

C. EXPERIMENTS ON PLATFORM
1) CUT-OFF FREQUENCY IDENTIFICATION
The PMSM used here is a laboratory-scale three-phase motor, the parameters of which are given in Table 1 and were obtained from the nameplate of the selected motor. Figure 8 shows the experimental curves for the cut-off frequency experiment. The cutoff frequency experiment was used to design the period and length of the PRBS signal. Different motor output velocity can be obtained by inputting different
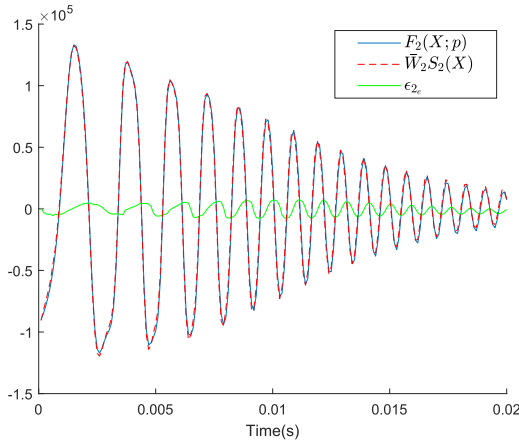
(a) Function approximation: $F_2(X;p)$
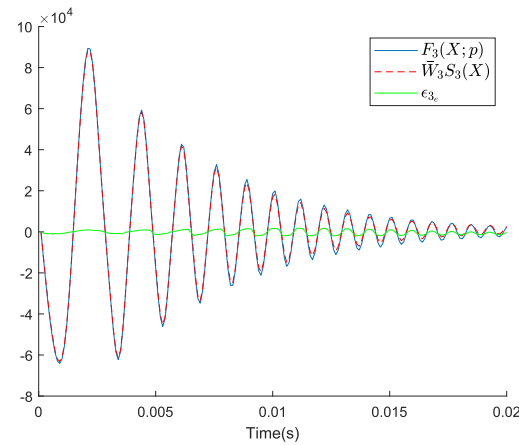
(b) Function approximation: $F_3(X;p)$

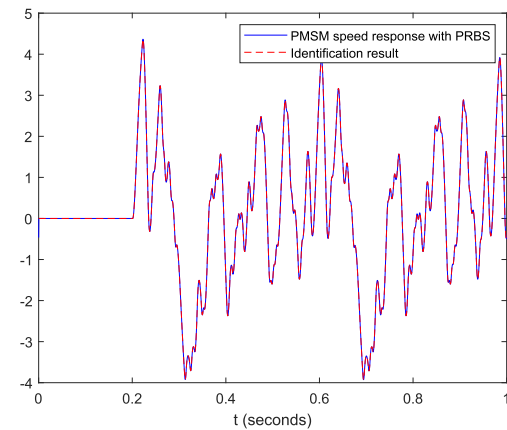**FIGURE 5.** The identification results of system dynamics.

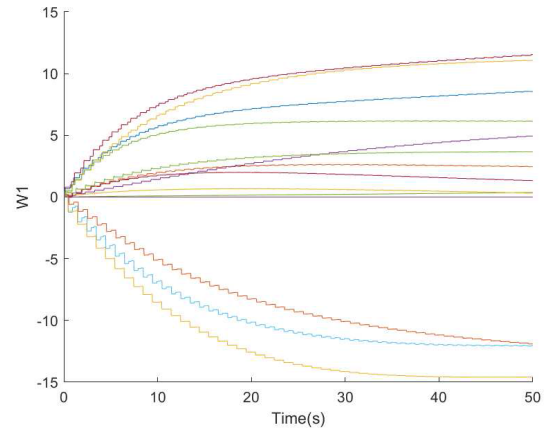**FIGURE 6.** Comparison between simulation data and identification results.

FIGURE 7. The convergence of the neural networks weights.

(a) The input of square wave.

(b) The real-time experiment response of the PMSM with t_s=0.0125s.

FIGURE 8. The experimental signals for cut-off frequency identification.

periods of the voltage square wave t_s on the experimental platform. When the motor speed output is almost zero, the reciprocal $1/t_s$ of the period of the square wave is the cutoff frequency of the motor system. Figure 8 shows the real-time PMSM velocity response of a square-wave input signal with a voltage amplitude of 310 V and $t_{sM} = 0.0125$ s period
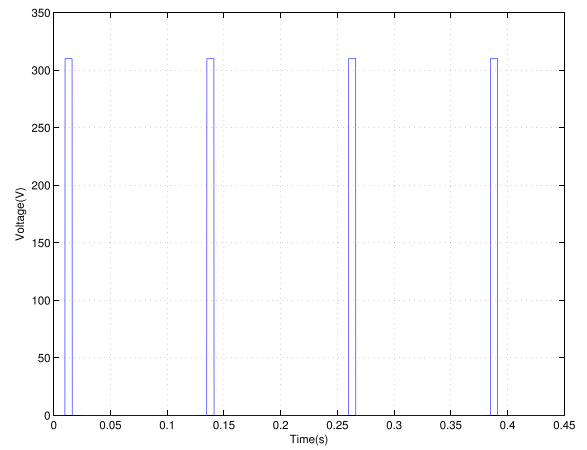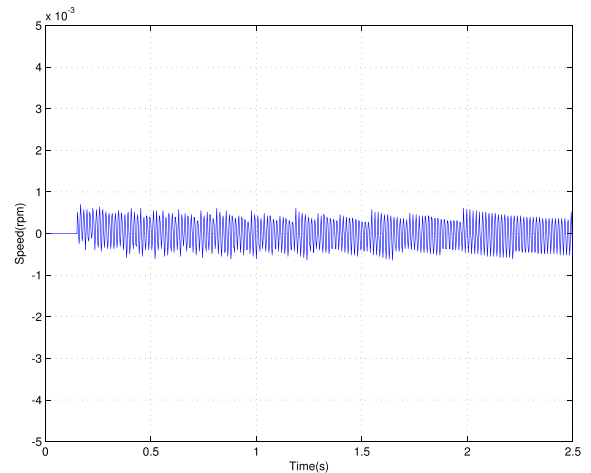
excitation. Therefore, the velocity response value is close to zero, and the cutoff frequency f_M is 80 Hz.

2) PRBS INPUT SIGNAL SELECTION FOR SYSTEM IDENTIFICATION

The pseudo-random binary sequence (PRBS) signal is often used as an input signal for system identification. The PRBS
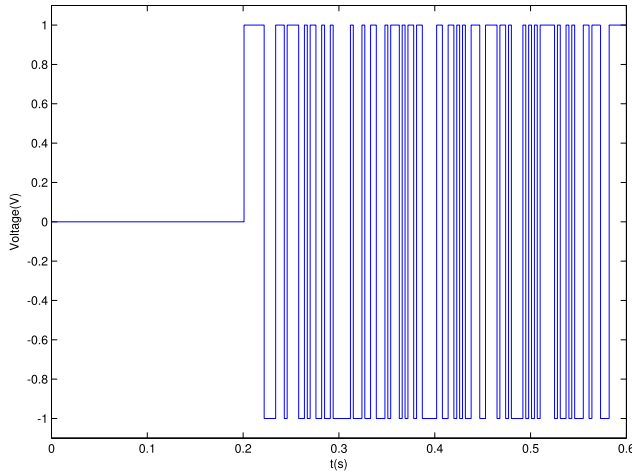
FIGURE 9. The input of PRBS in simulation and experimental set-up.

signal is a step function generated by a series of shift registers with an XOR operator. The maximum length PRBS signal has a correlation function similar to the white noise correlation function. This property does not hold for non-maximum length sequences. Therefore, the PRBS signal used in the identification process should be the maximum length PRBS signal. In order to design an effective PRBS test sequence, the period and length must be selected correctly. The determination of PRBS with a period of Δ and length N_p should follow the rules:

$$
\begin{cases}
\Delta \leq \dfrac{0.3}{f_M} \\
N_p \in [\dfrac{1.2}{f_M \cdot \Delta}, \quad \dfrac{1.5}{f_M \cdot \Delta}]
\end{cases}
\tag{21}
$$

where f_M is the system cut-off frequency.

Then it is easy to determine the PRBS input signal with a period of $\Delta = 0.003s$ and a length of $N_p = 127$ according to Eq. (21). By applying this input PRBS sequence, the PMSM velocity system can be fully stimulated to achieve accurate identification of system model behavior. Figure 9 shows the PRBS input used in the simulation and experiment.

3) EXPERIMENTAL RESULTS

In this subsection, we will evaluate the proposed method by using the experimental data from the PMSM platform. Injecting a PRBS input signal to the motor system from 0.2s (as shown in Figure 9), the velocity response exhibits periodic characteristics since the nature of the input PRBS is a periodic signal. The data is sampled by the DSP controller with a period of 0.0025 seconds as shown in Figure 10. It can be seen that from the time 0 to 0.2 seconds, the motor velocity is affected by noise and various uncertainties, which is different from the situation in the simulation. The response curve is shown in the blue line in Figure 10, and the system identification curve is shown in the red line.
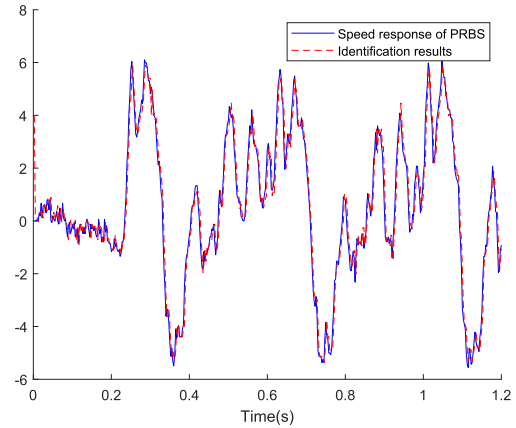

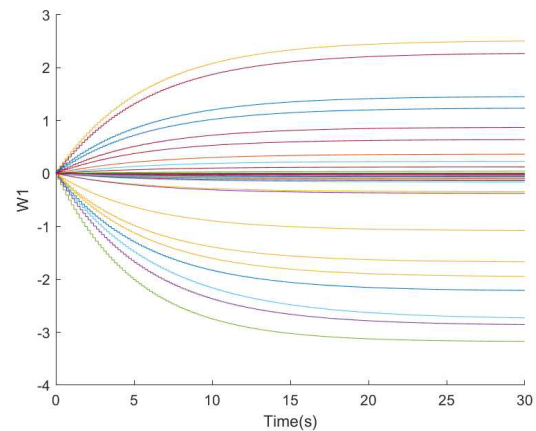FIGURE 10. Comparison between experimental and identification results.

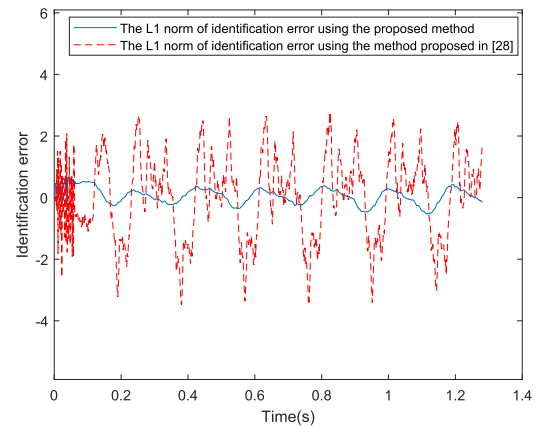FIGURE 11. The convergence of the neural networks weights.

FIGURE 12. The L1 norm of identification error.

Figure 11 shows the convergence of the neural network weights.

To demonstrate the advantages of the method, the PRBS response curve shown in Figure 10 was also identified using the identification method of [28] under the same experimental platform. Figure 12 gives the L1 norm of the identification error using the methods proposed in this paper and reference [28], which shows that the approach of this paper works better.

VI. CONCLUSION

In this study, a novel method via deterministic learning is proposed for identifying the PMSM velocity servo system. It achieves an accurate identification of the PMSM dynamics only based on system states. It is an advancement to use the system state for the identification of real PMSM system from the viewpoint of practical application. The effectiveness and feasibility of the proposed method are demonstrated from the numerical simulation and practical experiment. Different from existing methods in the literature, the identification result contains information about system parameters, various uncertainties, and system structure. Especially, it can be represented and stored in a constant manner, which makes it useful for recognizing similar dynamic behaviors for fault diagnosis or control design.

REFERENCES

[1] K. Liu, C. Hou, and W. Hua, "A novel inertia identification method and its application in pi controllers of pmsm drives," *IEEE Access*, vol. 7, pp. 13445–13454, 2019.

[2] J.-P. Louis, *control Synchronous Motors*. Hoboken, NJ, USA: Wiley, 2013.

[3] N. Imai, S. Morimoto, M. Sanada, and Y. Takeda, "Influence of magnetic saturation on sensorless control for interior permanent-magnet synchronous motors with concentrated windings," *IEEE Trans. Ind. Appl.*, vol. 42, no. 5, pp. 1193–1200, Sep. 2006.

[4] D. P. Marcetic and S. N. Vukosavic, "Speed-sensorless AC drives with the rotor time constant parameter update," *IEEE Trans. Ind. Electron.*, vol. 54, no. 5, pp. 2618–2625, Oct. 2007.

[5] B. Nahid-Mobarakeh, F. Meibody-Tabar, and F.-M. Sargos, "Mechanical sensorless control of PMSM with online estimation of stator resistance," *IEEE Trans. Ind. Appl.*, vol. 40, no. 2, pp. 457–471, Mar. 2004.

[6] M. Rashed, P. F. A. MacConnell, A. F. Stronach, and P. Acarnley, "Sensorless Indirect-Rotor-Field-Orientation speed control of a permanent-magnet synchronous motor with stator-resistance estimation," *IEEE Trans. Ind. Electron.*, vol. 54, no. 3, pp. 1664–1675, Jun. 2007.

[7] G. Gatto, I. Marongiu, and A. Serpi, "Discrete-time parameter identification of a surface-mounted permanent magnet synchronous machine," *IEEE Trans. Ind. Electron.*, vol. 60, no. 11, pp. 4869–4880, Nov. 2013.

[8] P.-Y. Chen, K.-H. Chao, and Y.-C. Tseng, "A motor fault diagnosis system based on cerebellar model articulation controller," *IEEE Access*, vol. 7, pp. 120326–120336, 2019.

[9] Y. Shi, K. Sun, L. Huang, and Y. Li, "Online identification of permanent magnet flux based on extended Kalman filter for IPMSM drive with position sensorless control," *IEEE Trans. Ind. Electron.*, vol. 59, no. 11, pp. 4169–4178, Nov. 2012.

[10] C. Moon and Y. A. Kwon, "Sensorless speed control of permanent magnet synchronous motor by unscented Kalman filter using various scaling parameters," *J. Electr. Eng. Technol.*, vol. 11, no. 2, pp. 347–352, Mar. 2016.

[11] H.-W. Sim, J.-S. Lee, and K.-B. Lee, "On-line parameter estimation of interior permanent magnet synchronous motor using an extended Kalman filter," *J. Electr. Eng. Technol.*, vol. 9, no. 2, pp. 600–608, Mar. 2014.

[12] X. Sun, C. Hu, G. Lei, Y. Guo, and J. Zhu, "State feedback control for a PM hub motor based on gray wolf optimization algorithm," *IEEE Trans. Power Electron.*, vol. 35, no. 1, pp. 1136–1146, Jan. 2020.

[13] X. Sun, Z. Jin, Y. Cai, Z. Yang, and L. Chen, "Grey wolf optimization algorithm based state feedback control for a bearingless permanent magnet synchronous machine," *IEEE Trans. Power Electron.*, vol. 35, no. 12, pp. 13631–13640, Dec. 2020.

[14] Z.-H. Liu, H.-L. Wei, Q.-C. Zhong, K. Liu, X.-S. Xiao, and L.-H. Wu, "Parameter estimation for VSI-fed PMSM based on a dynamic PSO with learning strategies," *IEEE Trans. Power Electron.*, vol. 32, no. 4, pp. 3154–3165, Apr. 2017.

[15] Z.-H. Liu, H.-L. Wei, Q.-C. Zhong, K. Liu, and X.-H. Li, "GPU implementation of DPSO-RE algorithm for parameters identification of surface PMSM considering VSI nonlinearity," *IEEE J. Emerg. Sel. Topics Power Electron.*, vol. 5, no. 3, pp. 1334–1345, Sep. 2017.

[16] Y. Xu, N. Parspour, and U. Vollmer, "Torque ripple minimization using online estimation of the stator resistances with consideration of magnetic saturation," *IEEE Trans. Ind. Electron.*, vol. 61, no. 9, pp. 5105–5114, Sep. 2014.

[17] K. Liu and Z. Q. Zhu, "Quantum genetic algorithm-based parameter estimation of PMSM under variable speed control accounting for system identifiability and VSI nonlinearity," *IEEE Trans. Ind. Electron.*, vol. 62, no. 4, pp. 2363–2371, Apr. 2015.

[18] K. Liu and Z. Q. Zhu, "Position-Offset-Based parameter estimation using the adaline NN for condition monitoring of permanent-magnet synchronous machines," *IEEE Trans. Ind. Electron.*, vol. 62, no. 4, pp. 2372–2383, Apr. 2015.

[19] K. Liu, Z. Q. Zhu, and D. A. Stone, "Parameter estimation for condition monitoring of PMSM stator winding and rotor permanent magnets," *IEEE Trans. Ind. Electron.*, vol. 60, no. 12, pp. 5902–5913, Dec. 2013.

[20] J. Yang, W.-H. Chen, S. Li, L. Guo, and Y. Yan, "Disturbance/Uncertainty estimation and attenuation techniques in PMSM Drives—A survey," *IEEE Trans. Ind. Electron.*, vol. 64, no. 4, pp. 3273–3285, Apr. 2017.

[21] C. Wang and D. J. Hill, "Learning from neural control," *IEEE Trans. Neural Netw.*, vol. 17, no. 1, pp. 130–146, Jan. 2006.

[22] C. Wang and D. J. Hill, "Deterministic learning and rapid dynamical pattern recognition," *IEEE Trans. Neural Netw.*, vol. 18, no. 3, pp. 617–630, May 2007.

[23] S. Luo and R. Gao, "Chaos control of the permanent magnet synchronous motor with time-varying delay by using adaptive sliding mode control based on DSC," *J. Franklin Inst.*, vol. 355, no. 10, pp. 4147–4163, Jul. 2018.

[24] Z. Li, J. Bae Park, Y. Hoon Joo, B. Zhang, and G. Chen, "Bifurcations and chaos in a permanent-magnet synchronous motor," *IEEE Trans. Circuits Syst. I, Fundam. Theory Appl.*, vol. 49, no. 3, pp. 383–387, Mar. 2002.

[25] M. Zribi, A. Oteafy, and N. Smaoui, "Controlling chaos in the permanent magnet synchronous motor," *Chaos, Solitons Fractals*, vol. 41, no. 3, pp. 1266–1276, Aug. 2009.

[26] C. Wang and D. J. Hill, *Deterministic Learning theory for Identification, Recognition, Control*. Boca Raton, FL, USA: CRC Press, 2009.

[27] G. Zhou and C. Wang, "Deterministic learning from control of nonlinear systems with disturbances," *Prog. Natural Sci.*, vol. 19, no. 8, pp. 1011–1019, Aug. 2009.

[28] W. Yu, Y. Luo, and Y. Pi, "Fractional order modeling and control for permanent magnet synchronous motor velocity servo system," *Mechatronics*, vol. 23, no. 7, pp. 813–820, Oct. 2013.

[29] W. Yu, Y. Chen, Y. Luo, and Y. Pi, "Frequency domain modelling and control of fractional-order system for permanent magnet synchronous motor velocity servo system," *IET Control Theory Appl.*, vol. 10, no. 2, pp. 136–143, Jan. 2016.

WEI YU received the M.S. and Ph.D. degrees from the School of Automation Science and Engineering, South China University of Technology, Guangzhou, China, in 2009 and 2014, respectively. From 2014 to 2016, he was a Postdoctoral Researcher with the Guangdong University of Technology, Guangzhou. He is currently a Lecturer with the School of Mechatronic Engineering and Automation, Foshan University, China. His research interests include fractional calculus, system identification, and fault diagnosis.

HENGHUI LIANG was born in Zhaoqing, Guangdong, China, in 1996. He is currently pursuing the master's degree in control engineering with Foshan University, Foshan, China. His research interests include the system modeling and control of permanent magnet synchronous motor.

XUNDE DONG received the M.Sc. degree in mathematical and applied mathematical and the Ph.D. degree in control theory and control engineering from the South China University of Technology, Guangzhou, China, in 2010 and 2014, respectively. He is currently an Assistant Professor with the School of Automation Science and Engineering, South China University of Technology. His research interests include distributed parameter systems, nonlinear adaptive control, and dynamical pattern recognition.

YING LUO (Member, IEEE) received the Ph.D. degree following a successive postgraduate-doctoral program in automation science and engineering from the South China University of Technology, Guangzhou, China, in 2009. He was an Exchange Ph.D. Student with the Center for Self-Organizing and Intelligent Systems, Department of Electrical and Engineering, Utah State University, Logan, UT, USA, from 2007 to 2009. He is currently a Full Professor with the Department of Mechanical Science and Engineering, Huazhong University of Science and Technology, Wuhan, China. His current research interests include applied fractional calculus in modeling and controls, high-accuracy motion controls, vibration isolation control, iterative and repetitive learning controls, and adaptive control. Together with Dr. Y. Chen, he has authored a research monograph entitled *Fractional Order Motion Controls* by John Wiley & Sons, Inc.

● ● ●